HHS Public Access

Author manuscript

Genes Chromosomes Cancer. Author manuscript; available in PMC 2019 December 01.

Published in final edited form as:

Genes Chromosomes Cancer. 2018 December ; 57(12): 611–621. doi:10.1002/gcc.22671.

A novel group of spindle cell tumors defined by S100 and CD34 co-expression shows recurrent fusions involving RAF1, BRAF, and NTRK1/2 genes

Albert J. H. Suurmeijer[1], **Brendan C. Dickson**[2], **David Swanson**[2], **Lei Zhang**[3], **Yun-Shao Sung**[3], **Paolo Cotzia**[3], **Christopher D. M. Fletcher**[4], **Cristina R. Antonescu**[3]

[1]Department of Pathology, University Medical Center, Groningen, University of Groningen, Groningen, The Netherlands [2]Department of Pathology and Laboratory Medicine, Mount Sinai Hospital, Toronto, Ontario, Canada [3]Department of Pathology, Memorial Sloan Kettering Cancer Center, New York, New York [4]Department of Pathology, Brigham and Women's Hospital, Harvard Medical School, Boston, Massachusetts

Abstract

Tumors characterized by co-expression of S100 and CD34, in the absence of SOX10, remain difficult to classify. Triggered by a few index cases with monomorphic cytomorphology and distinctive stromal and perivascular hyalinization, immunopositivity for S100 and CD34, and *RAF1* and *NTRK1* fusions, the authors undertook a systematic review of tumors with similar features. Most of the cases selected were previously diagnosed as low-grade malignant peripheral nerve sheath tumors, while others were deemed unclassified. The tumors were studied with targeted RNA sequencing and/or FISH. A total of 25 cases (15 adults and 10 children) with kinase fusions were identified, including 8 cases involving *RAF1*, 2 *BRAF*, 14 *NTRK1*, and 1 *NTRK2* gene rearrangements. Most tumors showed a monomorphic spindle cell proliferation with stromal and perivascular keloidal collagen, in a patternless architecture, with only occasional scattered pleomorphic or multinucleated cells. Most cases showed low cellularity, a low mitotic count, and absence of necrosis. Although a subset showed overlap with lipofibromatosis-like neural tumors, the study group showed distinctive hyalinization and overt malignant features, such as highly cellular fascicular growth and primitive appearance. All tumors showed co-expression of S100 and CD34, ranging from focal to diffuse. SOX10 was negative in all cases. NTRK1 immunohistochemistry showed high levels of expression in all tumors with *NTRK1* gene rearrangements. H3K27me3 expression performed in a subset of cases was retained. These findings together with the recurrent gene fusions in *RAF1*, *BRAF*, and *NTRK1/2* kinases suggest a distinct molecular tumor subtype with consistent S100 and CD34 immunoreactivity.

Correspondence: Cristina R. Antonescu, Department of Pathology, Memorial Sloan Kettering Cancer Center, 10021, New York, NY. antonesc@mskcc.org.

CONFLICT OF INTEREST

None.

Keywords

BRAF; CD34; fusions; NTRK1; NTRK2; RAF1; S100; sarcoma

1 | INTRODUCTION

Recurrent fusions involving genes encoding receptor tyrosine or cytoplasmic kinases have been described in distinct soft tissue tumors with spindle cell morphology and fibroblastic or neural differentiation.[1–4] The clinical importance of the oncogenic gene fusions involving kinases in these tumors is twofold. First, they may serve as molecular diagnostic markers in the classification of spindle cell sarcomas with overlapping morphology and a nonspecific immunoprofile. Second, several of these oncogenic kinases have been shown to be therapeutically targetable, which may potentially translate into better treatment strategies and improved patient outcome.[5–8] The correlation between various kinase fusions and different histologic subtypes is still evolving in soft tissue neoplasia and their specificity remains uncertain. It is unclear if the presence of these kinase fusions will span across tumors with different histologic grades or lines of differentiation.

Despite major advances in classification of soft tissue tumors with the increasing application of genomic tools in clinical practice, some lesions remain unclassified. Especially challenging are tumors with an ambiguous immunoprofile, such as tumors co-expressing S100 protein and CD34, in the absence of SOX10 reactivity. Prompted by detection of *RAF1* and *NTRK1* fusions in a group of tumors with monomorphic cytomorphology and co-expression of S100 and CD34, somewhat reminiscent of low-grade malignant peripheral nerve sheath tumors (MPNST), we mined our pathology department and consultation files at the contributing institutions for additional similar cases. Using a number of complementary molecular methods for fusion discovery and detection, including targeted RNA sequencing and FISH, we undertook a detailed pathologic characterization of a group of tumors sharing gene rearrangements in *RAF1*, *BRAF*, *NTRK1*, and *NTRK2*, which were previously labeled as MPNST or placed in the unclassified spindle cell sarcoma category.

2 | MATERIALS AND METHODS

2.1 | Cases

The study was triggered by 2 index cases with *RAF1* or *NTRK1* fusions which showed similar morphologic features and an identical immunoprofile of S100 and CD34 positivity. Thus the selection criteria were based on the light microscopic features of these index cases showing uniform spindle cell phenotypes with patternless architecture and band-like, keloidal stromal, and perivascular deposition of compact collagen. An immunoprofile of S100/CD34 co-expression, while lacking SOX10 staining, was also required for inclusion in the series. Using these strict criteria, a series of 20 cases of predominantly monomorphic, spindle cell tumors were selected from our archival and consultation files. Database searches were performed focusing on a previous diagnosis of low-grade or intermediate-grade MPNST or unclassified atypical/low-grade spindle cell tumors with co-expression of S100 and CD34 markers. Three additional cases were identified based on the presence of a kinase

fusion positive result, and subsequently included in the series as showing a similar morphologic spectrum and immunoprofile. An H3K27me3 was performed in a subset of cases with increased cellularity, mimicking MPNST. All confirmed cases had material for further molecular investigation. Medical charts were reviewed when available to exclude a history of NF1. Prototypical high-grade sarcomas or high-grade MPNSTs with high mitotic count, geographic areas of necrosis, and loss of H3K27me3 were excluded, as were MPNST cases associated with NF1 or previous radiation. A high-power field (HPF) was defined at ×400 magnification (0.237 mm^2 field of view) using an Olympus BX51 microscope (Olympus, Tokyo, Japan) with a standard eyepiece of 22 mm diameter. None of the tumors showed evidence of a pre-existent benign peripheral nerve sheath tumor.

2.2 | Immunohistochemistry

Immunohistochemistry for CD34, S100, and SOX10 expression was performed in all selected cases, using previously described method.[2] In tumors with *NTRK*-related fusions, IHC staining for TrkA (NTRK1) was performed on 12 of the 14 *NTRK1*-rearranged tumors, mostly in retrospect after the identification of the positive results by FISH/RNA sequencing. We used a commercially available TrkA rabbit monoclonal antibody, clone EP1058Y (Abcam, Cambridge, MA) at a dilution of 1:1500. H3K27me3 expression was examined in morphologically malignant tumors, with a cellular fascicular growth. Staining was performed on a Leica-Bond-3 (Leica, Buffalo Grove, IL) or a Ventana Benchmark (Ventana Medical Systems, Tucson, AZ) automated immunostaining platform using a heat-based antigen retrieval method and high-pH buffer.

2.3 | Targeted RNA sequencing

Three cases were analyzed by targeted RNA sequencing (Table 1). RNA was extracted from FFPE tissue using Amsbio's ExpressArt FFPE Clear RNA Ready kit (Amsbio LLC, Cambridge, MA). Fragment length was assessed with an RNA 6000 chip on an Agilent Bioanalyzer (Agilent Technologies, Santa Clara, CA). RNA-seq libraries were prepared using 20–100 ng total RNA with the Trusight RNA Fusion Panel (Illumina, San Diego, CA). Targeted RNA sequencing was performed on an Illumina MiSeq platform. Reads were independently aligned with STAR (version 2.3) against the human reference genome (hg19) and analyzed by STAR-Fusion.

2.4 | Anchored multiplex RNA sequencing (Archer DX)

One case was studied by Anchored Multiplex RNA sequencing assay, the detailed procedure of which has been previously described.[9] Unidirectional gene-specific primers were designed to target specific exons in 62 genes known to be involved in oncogenic fusions in solid tumors. In brief, RNA was extracted from formalin-fixed paraffin-embedded (FFPE) specimens, followed by cDNA synthesis and library preparation. Anchored Multiplex polymerase chain reaction amplicons were sequenced on Illumina Miseq, and the data were analyzed using the Archer software.

2.5 | Fluorescence in situ hybridization

All cases were tested by FISH for *RAF1*, *BRAF*, *NTRK1*, *NTRK2*, *MET*, and *RET* gene abnormalities. For *NTRK1*-rearranged cases, we additionally used available BAC probes spanning or flanking *LMNA*, *TPR*, and *TPM3* genes.[2] Custom probes were made by bacterial artificial chromosomes (BAC) clones flanking the genes of interest according to UCSC genome browser (http://genome.ucsc.edu) and obtained from BACPAC sources of Children's Hospital of Oakland Research Institute (Oakland, CA; http://bacpac.chori.org) (Supporting Information, Table S1).[4] DNA from each BAC was isolated according to the manufacturer's instructions. The BAC clones were labeled with fluorochromes (fluorescent-labeled dUTPs, Enzo Life Sciences, New York, NY) by nick translation and validated on normal metaphase chromosomes. The 4-μm-thick FFPE slides were deparaffinized, pretreated, and hybridized with denatured probes. After overnight incubation, the slides were washed, stained with 4′,6-diamidino-2-phenylindole, mounted with an antifade solution, and then examined on a Zeiss fluorescence microscope (Zeiss Axioplan, Oberkochen, Germany) controlled by Isis 5 software (Metasystems).

3 | RESULTS

3.1 | Tumors having overlapping histologic features with distinctive stromal keloidal and perivascular collagen deposition show recurrent *RAF1*, *BRAF*, and *NTRK1/2* rearrangements

The study cohort was defined by a histologic spectrum of monomorphic spindle cell phenotype with distinctive stromal and perivascular band-like hyalinization, typically arranged in a patternless fashion with an occasional/focal component of pleomorphic or multinucleate cells. The tumors revealed a variable degree of cellularity, most displaying a low cellularity and low mitotic count, but a subset showing clearly malignant features, with hypercellularity, fascicular growth, and increased mitotic activity. All tumors showed S100 and CD34 co-expression, ranging from patchy/multifocal to diffuse and strong, but were consistently negative for SOX10. The overall molecular findings identified 8 cases positive for *RAF1*, 2 with *BRAF*, 14 for *NTRK1*, and 1 for *NTRK2* gene rearrangements (Table 1).

3.2 | *RAF1* and *BRAF* fusion-positive tumors

Among the 8 *RAF1*-positive tumors, 2 presented in children (2 and 10 years of age) and 6 occurred in adult patients (age range 27–67 years). Both sexes were affected (5 females and 3 males). Five tumors were located on the trunk, one intra-abdominal (which involved stomach and pancreas), one visceral (rectum), and one extremity. The two *BRAF*-positive tumors were located in the palm of the hand of a 48-year-old female and the thigh of an 18-year-old female. Microscopically, all except one of the *RAF1*/*BRAF* fusion-positive tumors showed an infiltrative growth pattern within subcutaneous fat, skeletal muscle, and viscera. The tumors showed predominantly bland spindle morphology with a patternless architecture and scant mitotic activity. A striking feature was the pattern of stromal collagen deposition, which included keloidal bands and perivascular rings, encountered in 9/10 tumors (Figures 1 and 2). However, the tumors in this genetic group spanned a morphologic spectrum. At one end of the spectrum were tumors with atypical or low-grade features, characterized by low cellularity, mostly monomorphic cytology, and low mitotic activity. At the opposite end of

the spectrum were cases with an overtly malignant phenotype, showing marked increased cellularity, moderate increased mitotic activity, but lacked necrosis. Six *RAF1*/*BRAF* rearranged tumors had pure low-grade morphology with low cellularity and abundant collagenous stroma, and a low mitotic count (1–2 MF/10 HPFs) and lacked necrosis. One tumor each with *RAF1*/*BRAF* gene abnormalities (case 1 and 10) showed hybrid morphology, with low-grade areas that were mostly sharply demarcated from areas of increased cellularity and fascicular growth (Figures 1 and 2). The latter component was composed of primitive monomorphic spindle cells with scant cytoplasm and fusiform nuclei, with scant collagenous stroma, which in a three-tier grading system would fit best as an intermediate histologic grade sarcoma. Two additional cases showed increased cellularity and a moderate increase in mitotic activity (5–7 MF/10HPFs, cases # 6, 8; Table 1). None of the tumors from the *RAF1*/*BRAF*-positive group showed the presence of lipofibromatosis-like areas, while focal pleomorphic or multinucleated cells were present in only one of the *BRAF*-rearranged cases (case 9, Figure 2).

Follow-up was available in 6 of the 10 cases. Among the 6 cases with low cellularity/pure low-grade tumors, follow-up was available in half of them; 2 patients were with no evidence of disease (NED) and 1 had persistent local disease in the hand after 22 months follow-up (case 9), as it was originally excised with positive margins (Table 1). From the 4 cases with malignant phenotype (increased cellularity and mitotic activity), follow-up was available in 3 cases, showing 2 patients with NED after 9 and 25 months, respectively. The latter patient (case 8) had an initial incomplete resection, followed by re-excision and radiation therapy. The third patient (Case 1), a 67-year-old female with a large 15 cm upper intra-abdominal mass, infiltrating stomach and pancreas, developed numerous lung, liver, and intraperitoneal metastases and was alive with disease after 7 months follow-up. This tumor was also the only case from the entire cohort which showed focal areas of heterologous chondroid matrix deposition (Figure 1).

The 3 *RAF1*-positive tumors studied with an RNAseq platform revealed 3 different gene fusion partners, including *PDZRN3*, *SLMAP*, and *TMF1*, all being located on chromosome 3 (Table 1). In the 2 cases tested, targeted RNA sequencing identified an in-frame fusion of *RAF1* exon 8 to either *PDZRN3* exon 5 or *SLMAP* exon 10 (on p25.2), respectively (Figure 3). In case #1, *PDZRN3* (3p13) and *RAF1* (3p25.2) genes shared the same direction of transcriptions, the fusion resulting from a t(3;3)(p13;p25) translocation. In case#2, *SLMAP* gene (3p14.3) was in opposite direction of transcription to *RAF1*, thus the fusion was the result of an intrachromosomal inversion. The predicted fusion oncoproteins included the kinase domain of *RAF1*, encoded by exons 8–17 (Figure 3). Interestingly, by unsupervised hierarchical clustering using the same platform of targeted RNA sequencing data of more than 100 various soft tissue tumors, these two *RAF1*-rearranged tumors clustered closely to a *BRAF*-rearranged pediatric fibrosarcoma, described in an earlier report by our group[4] (Figure 3). Among the various soft tissue tumor types included on the RNAseq platform are small blue round cell tumors with various gene fusions, infantile fibrosarcomas, synovial sarcomas, angiosarcoma, dermatofibrosarcoma protuberans, solitary fibrous tumors, ossifying fibromyxoid tumors, and unclassified sarcomas, NOS.

3.3 | *NTRK*-rearranged spindle cell tumors encompass a histologically diverse spectrum spanning low and high cellularity

There were 14 tumors with *NTRK1* rearrangements and one with *NTRK2*-related fusion (Table 1). Eight *NTRK1*-rearranged tumors presented in pediatric patients younger than 18 years of age (range 3–17, mean 11.3), whereas six tumors occurred in adults (age range 26–61 years). Two tumors originated in the jawbones, one in the mandible and the other in the maxilla. Twelve tumors were soft tissue tumors, located in the extremities ($n = 8$), trunk ($n = 3$), or stomach (1 case). There was no gender predilection (8 males and 6 females). Overall the *NTRK1* group showed significant morphologic and IHC overlap with the tumors showing *RAF1* and *BRAF1* gene abnormalities, described above. Similarly, *NTRK1*-rearranged spindle cell tumors could roughly be divided in two groups. At one end of the spectrum, 12 cases were composed of low cellularity, predominantly monomorphic spindle cell proliferation with haphazardly growth. Within this lower grade group, 9 tumors had distinctive patterns of keloidal stromal collagen deposition and perivascular hyalinized rings (Figure 4). Three tumors had areas with scattered pleomorphic and multinucleate tumor cells (Figure 4). Four superficially located tumors showed reticular infiltration of subcutaneous fat, a morphology somewhat reminiscent of lipofibromatosis-like neural tumor (Figure 4). The mitotic index of these tumors was low, ranging 1–5 MF/10 HPFs. At the other end of the spectrum, three *NTRK1* rearranged spindle cell sarcomas were composed of cellular fascicular areas, with >10 MF/10 HPFs and lacked necrosis, which would correspond to an intermediate histo-logic grade category. One of these 3 lesions showed a sharply demarcated area of low grade morphology (Figure 4). Similar to *RAF1*/*BRAF* fusion-positive tumors, all *NTRK1*-positive tumors showed co-expression of CD34 and S100. In addition, these tumors diffusely expressed TRK-A in all 12 cases analyzed (Figure 4).

Clinical follow-up in this group was available in 8 of the 15 total patients from the *NTRK1/2* molecular group. Of the 11 low-grade lesions, follow-up was available in 5, all being NED after a median of 16 months (range 3–648 months, mean 165). One of these patients developed local recurrence and was subsequently treated with resection and radiation therapy, and is NED for 144 months (case 12). From the remaining 4 patients with a malignant phenotype (increased cellularity and/or increased mitotic activity), 3 had follow-up information showing an aggressive clinical course with development of distant metastases to the lung and other locations (Table 1, cases#14, 15, and 20).

The most common *NTRK1* fusion partner was *LMNA* gene present in 8 (57%) of 14 cases, followed by a *TPM3–NTRK1* fusion identified in 3 (21%) cases (Table 1). One of these cases were also validated by Archer DX, showing an in-frame fusion between *TPM3* exon 8 and *NTRK1* exon10, preserving the kinase domain (Supporting Information, Figure S1). Only one case showed a *TPR–NTRK1* gene fusion. In 2 cases, no *NTRK1* gene partner could be identified by FISH testing. None of the tumors in this series harbored *MET* or *RET* gene rearrangements.

One case showed the presence of a *SPECC1L–NTRK2* fusion by targeted RNA sequencing, which was further confirmed by FISH *NTRK2* break-apart assay (Figure 5). The tumor was associated with high levels of *NTRK2* mRNA expression, compared to other tumor types. The lesion occurred in a 20-year-old male with a forearm mass; the patient had a history of

severe trauma to the arm 1 year prior. Microscopically, the tumor had a similar morphologic appearance to all the other kinase fusion variants, of a low cellularity spindle cell tumor with a haphazard growth pattern, composed of mostly uniform cytomorphology and scattered plumper cells with enlarged and multilobated nuclei with smudgy chromatin. Distinctive stromal and perivascular thick, band-like collagen was also noted. The tumor also showed a focal lipofibromatosis-like component within the subcutaneous fat. The tumor showed diffuse reactivity for S100 and CD34, retained H3K27me3 expression and was negative for SOX10.

4 | DISCUSSION

In this study, we describe the clinicopathologic and molecular features of a series of 25 spindle cell neoplasms with recurrent *RAF1*, *BRAF*, and *NTRK1/2* gene rearrangements.

This is the first report of *RAF1* gene fusions in soft tissue tumors. RAF1 is a member of the *RAF* family of signaling kinases, downstream of *RAS*, which activate the *MEK–ERK* pathway that promotes cell proliferation and survival. Isolated examples of *RAF1* fusions have been reported in various epithelial malignancies, such as prostate, breast, thyroid, and pancreas,[10] as well as in a group of pediatric low-grade gliomas.[11] *RAF1*-related fusions, such as *BRAF* gene fusions have been reported in similar tumor types, for example, thyroid cancer and melanoma.[12–14] In addition, *BRAF* gene rearrangements have been described recently in a subset of spindle cell sarcomas, morphologically resembling infantile fibrosarcomas.[4] In that study, we identified 3 children, ranging from 6 months to 16 years old, with tumors occurring in the abdominal cavity (1 retroperitoneum and 2 pelvic). The morphologic appearance was characterized by primitive monomorphic spindle cells arranged in long, intersecting fascicles, associated with a variable hemangiopericytoma-like vascular pattern. The tumors showed no specific line of differentiation by immunohistochemistry, with only focal SMA reactivity seen in 2 cases tested. From the publicly available expression data, neither *BRAF*-fusion-positive carcinomas nor sarcomas appeared to be associated with *BRAF* mRNA upregulation.

Other established examples of recurrent kinase gene rearrangements in spindle cell tumors are *ETV6–NTRK3* fusions in infantile fibrosarcomas (IFS), sarcomas that typically present at birth or in the first 2 years of life.[1] Moreover, recurrent variant *NTRK1* fusions have been detected in the so-called lipofibromatosis-like neural tumors, which is another group of pediatric and young adult lesions, that, by immunohistochemistry (IHC), often co-express CD34 and S100 (but not SOX10), suggesting neural differentiation.[2] Lipofibromatosis-like neural tumors are characterized by a highly infiltrative growth pattern within adipose tissue, which can be difficult to distinguish from typical lipofibromatosis. In addition, four of our *NTRK1*-fusion-positive tumors with low-grade histology showed focal areas resembling lipofibromatosis. The exact relationship between this latter entity and the recent cohort of cases remains uncertain. Lipofibromatosis-like neural tumors share a similar immunoprofile, but typically lack overt malignant features and the distinctive band-like stromal or perivascular hyalinization present in this study, and so far have been related only to *NTRK1* gene fusions. Moreover, similar *NTRK1*-related fusions, including *LMNA* and *TPM3* gene partners, have been reported by Haller et al. in 4 tumors characterized by a prominent

myopericytic/hemangiopericytic pattern. In contrast to our cases, only 1 tumor was immunopositive for CD34, while S100 protein was not reported.[15] Although these tumors belong to the spectrum of spindle cell sarcomas with kinase fusion genes, we did not discern these growth patterns in any of the cases in this cohort.

A *STRN–NTRK2* fusion variant was reported in one pediatric patient with soft tissue sarcoma, although the exact morphologic features remain unclear.[8,16,17] The case showed a transcript composed of *STRN* exon 15 fused to *NTRK2* exon 4. We found an additional case in this study cohort displaying low cellularity and fibrotic stroma occurring in a 20-year-old male in the forearm, harboring a *SPECC1L–NTRK2* fusion (Figure 5) resulting from a t(9;22)(q21.33; q11.23) trans-location. The fusion retains the NTRK2 kinase domain in the predicted oncoprotein and shows high levels of mRNA overexpression compared to other sarcoma types.

Although the *RAF1*, *BRAF*, and *NTRK1/2*-rearranged tumors showed morphologic and immunophenotypic features suggestive of MPNST, the current series harbor certain differences from the prototypical low-grade and high-grade MPNST, in particular with respect to clinical context and IHC features. A diagnosis of low-grade MPNST is usually considered in tumors arising in patients with neurofibromatosis (NF1), representing malignant transformation in a pre-existent neurofibroma. Arbitrary consensus criteria on how to diagnose low-grade MPNST in this context were proposed recently.[18] Importantly, low-grade MPNST contains numerous S100-positive and SOX10-positive Schwann cells, while losing most of the intermixed CD34-positive fibroblastic framework stroma, which is typically retained in the preexistent neurofibroma component. In contrast, our study group with low-grade morphology showed co-expression of S100 and CD34, and consistently lacked SOX10 reactivity. Furthermore, none showed a neurofibroma component or had a history of NF1. On the other hand, high-grade MPNST can be sporadic, NF1-associated, or occur in the field of prior radiation. Up to 40% of high-grade MPNST focally express nerve sheath markers S100 and GFAP, and about 50% show focal nuclear SOX10 expression.[19] The large majority of high-grade MPNST shows diffuse loss of trimethylation of H3K27, which remains a useful diagnostic IHC marker.[20,21] Notably, the *NTRK1* and *RAF1*/*BRAF*-rearranged tumors with increased cellularity and fascicular growth in this series were positive for S100 and CD34, negative for SOX10, and retained H3K27me3 expression. A somewhat controversial entity is the so-called “fibroblastic MPNST,” a tumor that also shows co-expression of CD34 and S100.[22,23] Mills et al.[22] described three uterine sarcomas, two of which presented in women under the age of 35 years, and which they designated endocervical fibroblastic MPNST. These tumors were composed of spindle cells with a cellular fascicular, storiform, and whorled architecture. The high-grade microscopic features of these sarcomas translated into biologic behavior, with one tumor that recurred locally and one that developed distant metastases. In the case report by Houreih et al.,[23] a 11 cm retroperitoneal tumor occurring in a 29-year-old male was composed of monomorphic spindle cells with patternless and fascicular architecture, with distinctive perivascular hyalinization and stromal collagen rosettes, matching quite well the findings of many of the low-grade MPNST-like tumors in our study group. It remains to be determined if cases previously designated as “fibroblastic MPNST” would be reclassified genetically as having *NTRK1/2* or *RAF1*/*BRAF* gene fusions.

Two spindle cell neoplasms in our cohort had *BRAF* rearrangements. *BRAF* fusions have also been reported in IFS-like sarcomas.[4] Interestingly, by whole transcriptome analysis, two of the *RAF1*-rearranged tumors in this series clustered with one of the *BRAF* rearranged IFS-like pediatric tumors. Fascicular spindle cell sarcomas with *NTRK1* rearrangements and similar fibrosarcoma-like morphology have been described in soft tissue and uterus in previous publications from our group.[4,24] Given these observations, it seems reasonable to assume that *RAF1*/*BRAF* and *NTRK1* kinase fusion-associated tumors, including the lesions from the present series and the IFS-like, might be closely related.

The histology of the tumors in the current series, with patternless growth and stromal and perivascular collagen bands, is somewhat reminiscent of solitary fibrous tumor (SFT). However, grossly, SFT is a well-demarcated and encapsulated tumor, whereas *NTRK1/2* and *RAF1*/*BRAF*-rearranged tumors infiltrate subcutaneous fat or skeletal muscle fibers. By IHC, SFT is positive for CD34 in the majority of cases, but lacks S100 expression. Moreover, nearly all SFT have a *NAB2–STAT6* fusion[25] and STAT6 is a highly sensitive and specific IHC marker for SFT.[26,27] Other bland fibroblastic spindle cell tumors with collagen bands and perivascular collagen deposits and diffuse CD34 expression include cellular angiofibroma, mammary-type myofibroblastoma, and spindle cell lipoma, three tumors which are histogenetically related, as they all have abnormalities in 13q14, leading to loss of Rb1.[28] All these CD34 fibroblastic tumors are S100 protein negative.

Clinical follow-up, albeit limited, clearly emphasized that tumors with a malignant phenotype, defined by increased cellularity and mitotic activity, have the propensity for distant spread and follow an aggressive clinical course. In this respect, two recent clinical studies[8,17] demonstrated promising sensitivity of various malignancies with *TRK* fusions to Larotrectinib, a highly selective small molecule TRK inhibitor. One of the studies included 7 patients with infantile fibrosarcoma and 11 patients with other soft tissue sarcomas in advanced stage.[8] Detailed histology was not available, but the tumors had been diagnosed as spindle cell sarcoma, NOS, MPNST, myopericytoma/myofibroma, and inflammatory myofibroblastic tumor. Most of the sarcoma patients had a (durable) partial response, whereas only few had a complete response. Although tumor response was not related to *TRK* fusion type or cancer type, the longest response (27 months) was observed in a patient with an *LMNA–NTRK1* fusion-positive undifferentiated sarcoma that had metastasized to the lung.[29]

In conclusion, we describe a series of spindle cell tumors resembling low- to intermediate-grade MPNST, occurring in both children and young adults, in various anatomic sites (including bone, soft tissue, and viscera) and harboring recurrent gene fusions in various kinases, such as RAF1, BRAF, NTRK1, and NTRK2. Regardless of the different fusion variants, most tumors showed a monomorphic spindle cell histology, patternless growth, and distinctive band-like stromal hyalinization and perivascular collagen rings. Our findings suggest that these kinase fusions may define a novel tumor entity with *RAF1*, *BRAF*, and *NTRK1/2* fusions. However, despite rather uniform morphology and immunoprofile, the various genotypes span a broad spectrum of clinical behavior, with tumors of low cellularity showing an indolent course, while others with increased cellularity and mitotic activity being prone to distant metastasis and death from disease, based on our limited follow-up available.

These tumors should be distinguished from prototypical MPNST lesions, which often occur in the setting of NF1 or prior radiation, as they may be amenable to targeted therapy. Our results add this novel subtype to the growing list of soft tissue tumors characterized by oncogenic kinase activation through gene fusions. Furthermore, *NTRK1* immunohistochemistry appears to be a sensitive method to select this subset of tumors with *NTRK1* gene rearrangements.

Supplementary Material

Refer to Web version on PubMed Central for supplementary material.

ACKNOWLEDGMENTS

The authors thank the following pathologists and clinicians who kindly referred case material and provided clinical follow-up when available: Dr Steven Drexler, Mineola, NY; Dr Robert Maki, Lake Success, NY; Dr Lawrence Edusei, Accra, Ghana; Dr Muhammad Idrees, Indianapolis, IN; Dr Nicky Leeborg, Portland, OR; Prof. Jose Manuel Lopes, Porto, Portugal; Dr Ira Miller, Chicago, IL; Dr Alessandra Nascimento, Rio de Janeiro, Brazil; Dr Michael O'Malley, Baltimore, MD; Dr Mark Phillips, West Palm Beach, FL; Dr Andrew Rosenberg, Miami, FL; Prof. Dr Raf Sciot, Leuven, Belgium; Dr David Spence, Chattanooga, TN; Dr Ginger Holt, Nashville, TN; Dr Sara Szabo, Cincinnati, OH; Dr Toyohiro Tada, Aichi, Japan; Dr Bhumita Vadgama, Southampton, United Kingdom.

Supported in part by P50 CA140146-01 (CRA); P30-CA008748 (CRA); Kristen Ann Carr Foundation (CRA); Cycle for Survival (CRA).

Funding information

National Institute of Health; Kristen Ann Carr Foundation (CRA), Grant/Award Numbers: P30-CA008748, P50 CA140146-01

REFERENCES

1. Knezevich SR, McFadden DE, Tao W, Lim JF, Sorensen PH. A novel ETV6-NTRK3 gene fusion in congenital fibrosarcoma. Nat Genet. 1998;18:184–187. [PubMed: 9462753]
2. Agaram NP, Zhang L, Sung YS, et al. Recurrent NTRK1 gene fusions define a novel subset of locally aggressive lipofibromatosis-like neural tumors. Am J Surg Pathol. 2016;40:1407–1416. [PubMed: 27259011]
3. Pavlick D, Schrock AB, Malicki D, et al. Identification of NTRK fusions in pediatric mesenchymal tumors. Pediatr Blood Cancer. 2017;64: e26433.
4. Kao YC, Fletcher CDM, Alaggio R, et al. Recurrent BRAF gene fusions in a subset of pediatric spindle cell sarcomas: expanding the genetic spectrum of tumors with overlapping features with infantile fibrosarcoma. Am J Surg Pathol. 2018;42:28–38. [PubMed: 28877062]
5. Wong V, Pavlick D, Brennan T, et al. Evaluation of a congenital infantile fibrosarcoma by comprehensive genomic profiling reveals an LMNA-NTRK1 gene fusion responsive to Crizotinib. J Natl Cancer Inst. 2016;108:1–3.
6. Vaishnavi A, Le AT, Doebele RC. TRKing down an old oncogene in a new era of targeted therapy. Cancer Discov. 2015;5:25–34. [PubMed: 25527197]
7. Nagasubramanian R, Wei J, Gordon P, Rastatter JC, Cox MC, Pappo A. Infantile fibrosarcoma with NTRK3-ETV6 fusion successfully treated with the tropomyosin-related kinase inhibitor LOXO-101. Pediatr Blood Cancer. 2016;63:1468–1470. [PubMed: 27093299]
8. Drilon A, Laetsch TW, Kummar S, et al. Efficacy of larotrectinib in TRK fusion-positive cancers in adults and children. N Engl J Med. 2018;378: 731–739. [PubMed: 29466156]
9. Zheng Z, Liebers M, Zhelyazkova B, et al. Anchored multiplex PCR for targeted next-generation sequencing. Nat Med. 2014;20:1479–1484. [PubMed: 25384085]
10. Stransky N, Cerami E, Schalm S, Kim JL, Lengauer C. The landscape of kinase fusions in cancer. Nat Commun. 2014;5:4846. [PubMed: 25204415]

11. Jain P, Fierst TM, Han HJ, et al. CRAF gene fusions in pediatric low-grade gliomas define a distinct drug response based on dimerization profiles. Oncogene. 2017;36:6348–6358. [PubMed: 28806393]
12. Ciampi R, Knauf JA, Kerler R, et al. Oncogenic AKAP9-BRAF fusion is a novel mechanism of MAPK pathway activation in thyroid cancer. J Clin Invest. 2005;115:94–101. [PubMed: 15630448]
13. Wiesner T, He J, Yelensky R, et al. Kinase fusions are frequent in Spitz tumours and spitzoid melanomas. Nat Commun. 2014;5:3116. [PubMed: 24445538]
14. Ross JS, Wang K, Chmielecki J, et al. The distribution of BRAF gene fusions in solid tumors and response to targeted therapy. Int J Cancer. 2016;138:881–890. [PubMed: 26314551]
15. Haller F, Knopf J, Ackermann A, et al. Paediatric and adult soft tissue sarcomas with NTRK1 gene fusions: a subset of spindle cell sarcomas unified by a prominent myopericytic/haemangiopericytic pattern. J Pathol. 2016;238:700–710. [PubMed: 26863915]
16. Rudzinski ER, Lockwood CM, Stohr BA, et al. Pan-Trk immunohisto-chemistry identifies NTRK rearrangements in pediatric mesenchymal tumors. Am J Surg Pathol. 2018;42:927–935. [PubMed: 29683818]
17. Laetsch TW, DuBois SG, Mascarenhas L, et al. Larotrectinib for paediatric solid tumours harbouring NTRK gene fusions: phase 1 results from a multicentre, open-label, phase 1/2 study. Lancet Oncol. 2018;19:705–714. [PubMed: 29606586]
18. Miettinen MM, Antonescu CR, Fletcher CDM, et al. Histopathologic evaluation of atypical neurofibromatous tumors and their transformation into malignant peripheral nerve sheath tumor in patients with neurofibromatosis 1-a consensus overview. Hum Pathol. 2017;67:1–10. [PubMed: 28551330]
19. Nonaka D, Chiriboga L, Rubin BP. Sox10: a pan-schwannian and melanocytic marker. Am J Surg Pathol. 2008;32:1291–1298. [PubMed: 18636017]
20. Schaefer IM, Fletcher CD, Hornick JL. Loss of H3K27 trimethylation distinguishes malignant peripheral nerve sheath tumors from histologic mimics. Mod Pathol. 2016;29:4–13.
21. Prieto-Granada CN, Wiesner T, Messina JL, Jungbluth AA, Chi P, Antonescu CR. Loss of H3K27me3 expression is a highly sensitive marker for sporadic and radiation-induced MPNST. Am J Surg Pathol. 2016;40:479–489. [PubMed: 26645727]
22. Mills AM, Karamchandani JR, Vogel H, Longacre TA. Endocervical fibroblastic malignant peripheral nerve sheath tumor (neurofibrosarcoma): report of a novel entity possibly related to endocervical CD34 fibrocytes. Am J Surg Pathol. 2011;35:404–412. [PubMed: 21317712]
23. Houreih MA, Eyden B, Deolekar M, Banerjee S. A case of fibroblastic low-grade malignant peripheral nerve sheath tumor--a true neurofibrosarcoma. Ultrastruct Pathol. 2007;31:347–356. [PubMed: 17963184]
24. Chiang S, Cotzia P, Hyman DM, et al. NTRK fusions define a novel uterine sarcoma subtype with features of fibrosarcoma. Am J Surg Pathol. 2018;42:791–798. [PubMed: 29553955]
25. Robinson DR, Wu YM, Kalyana-Sundaram S, et al. Identification of recurrent NAB2-STAT6 gene fusions in solitary fibrous tumor by integrative sequencing. Nat Genet. 2013;45:180–185. [PubMed: 23313952]
26. Doyle LA, Vivero M, Fletcher CD, Mertens F, Hornick JL. Nuclear expression of STAT6 distinguishes solitary fibrous tumor from histologic mimics. Mod Pathol. 2014;27:390–395. [PubMed: 24030747]
27. Cheah AL, Billings SD, Goldblum JR, Carver P, Tanas MZ, Rubin BP. STAT6 rabbit monoclonal antibody is a robust diagnostic tool for the distinction of solitary fibrous tumour from its mimics. Pathology. 2014;46:389–395. [PubMed: 24977739]
28. Chen BJ, Marino-Enriquez A, Fletcher CD, Hornick JL. Loss of retinoblastoma protein expression in spindle cell/pleomorphic lipomas and cytogenetically related tumors: an immunohistochemical study with diagnostic implications. Am J Surg Pathol. 2012;36:1119–1128. [PubMed: 22790852]
29. Doebele RC, Davis LE, Vaishnavi A, et al. An oncogenic NTRK fusion in a patient with soft-tissue sarcoma with response to the tropomyosin-related kinase inhibitor LOXO-101. Cancer Discov. 2015;5:1049–1057. [PubMed: 26216294]

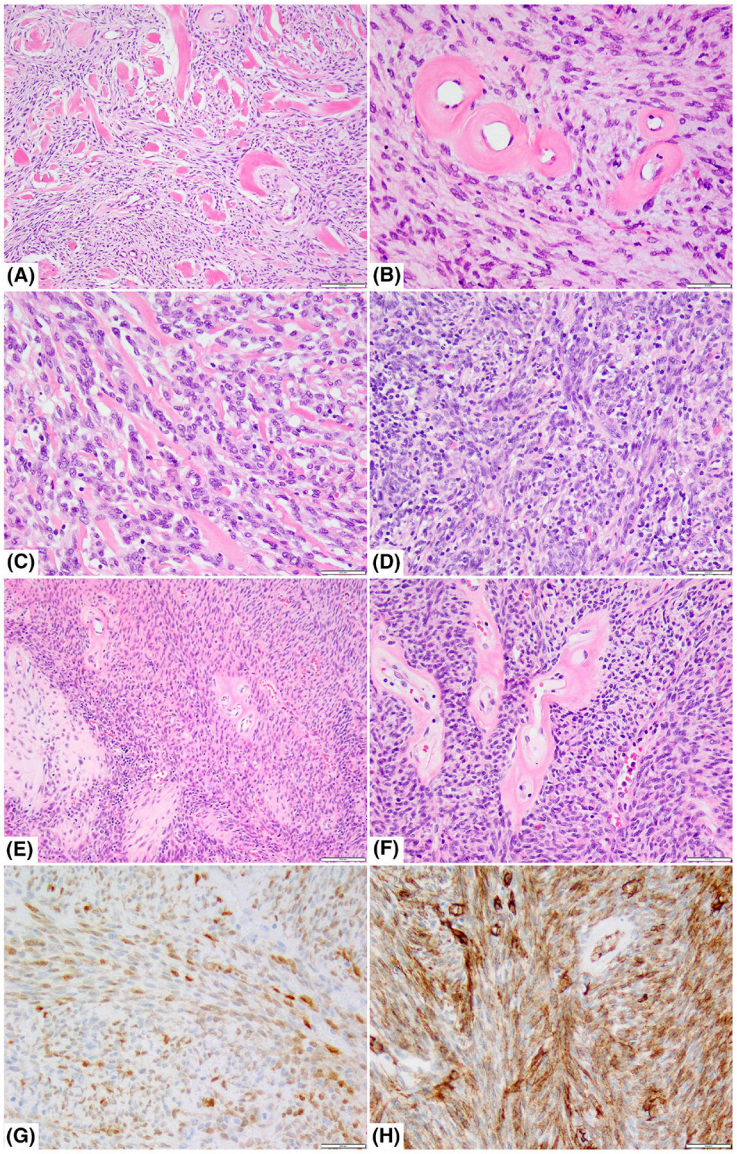

FIGURE 1.

Histologic and immunohistochemical features of *RAF1*-fusion-positive tumors. A,B, Deep seated paraspinal tumor in a 45-year-old female showing a moderately cellular haphazardly arranged spindle cell proliferation with prominent stromal hyaline collagen bands (case 4; A, ×40) and perivascular collagen rings (B; ×200); C, D. Chest wall tumor in a 59-year-old male showing monomorphic spindle cells streaming along bands of collagen (case 8; C; ×200) or containing scattered lymphocytes (D; ×200); E,F, A large intra-abdominal sarcoma infiltrating into pancreas and gastric wall in a 67-year-old female showing cellular fascicles of hyperchromatic spindle cells with foci of heterologous cartilage (case 1; E; ×40) and distinctive perivascular rings of collagen (F; ×200); immunohistochemistry performed in the same case showing multifocal weak S100 (G, ×100) and more diffuse, strong CD34 staining (H, ×100)

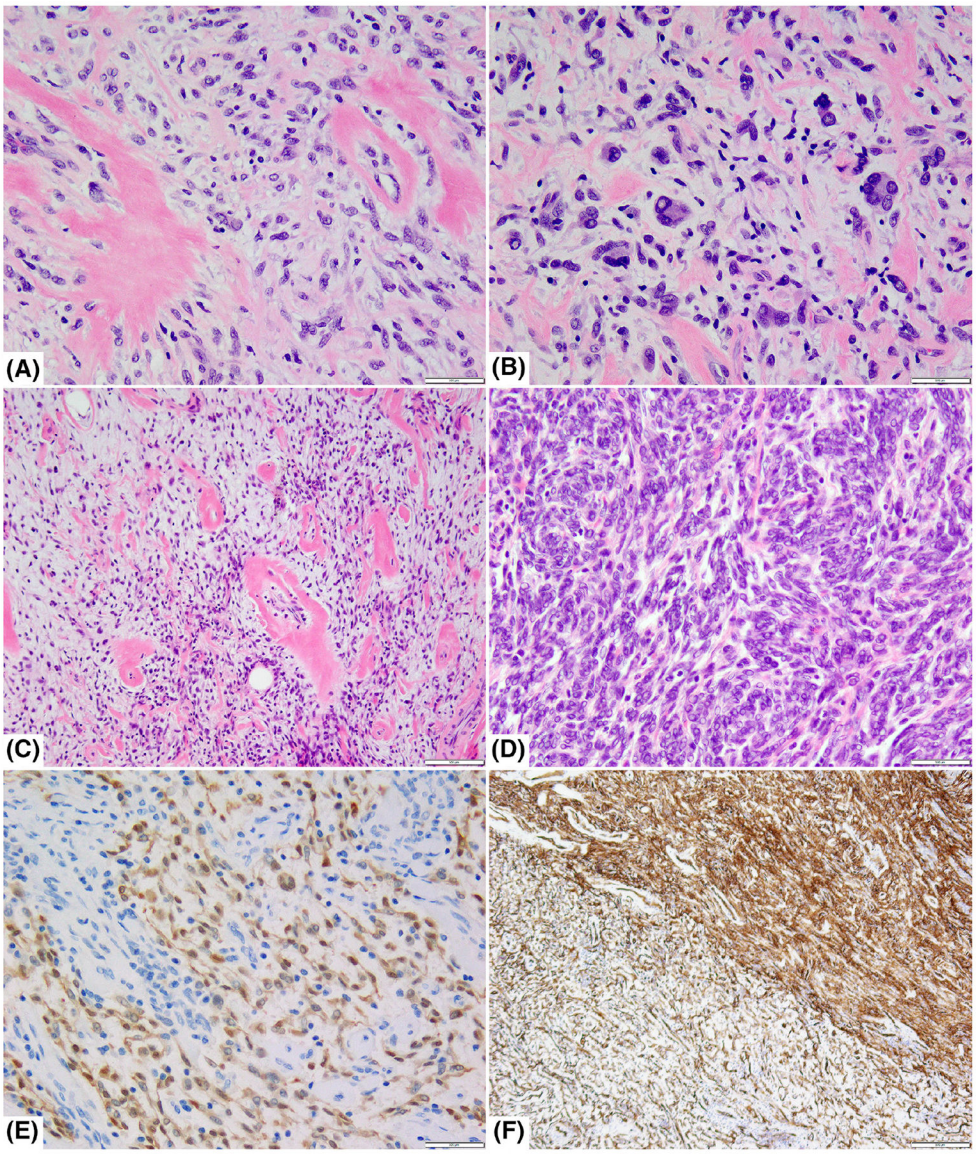

FIGURE 2.

Histologic and immunohistochemical features of tumors with *BRAF* gene rearrangements. A, Low cellularity lesion occurring in the hand soft tissue of a 48-year-old female showing a patternless growth of monomorphic spindle cells separated by “amianthoid-like” stromal collagen and perivascular rings. B, Same case showing focal areas with pleomorphic and multinucleate cells (case 9, ×200); C,D, A deep-seated thigh mass in a 18-year-old female showing hybrid low and increased cellularity with abrupt transition (case 10); the lower grade component showed typical perivascular dense hyalinization (C; ×100), while the cellular areas revealed primitive spindle blue cells arranged in short, intertwining fascicles (D; ×200); E,F, Immunohistochemistry performed on the same case showed patchy S100 staining (more pronounced in the low-grade areas) (E; ×200), while CD34 showed a more diffuse pattern in both components (F; ×40)

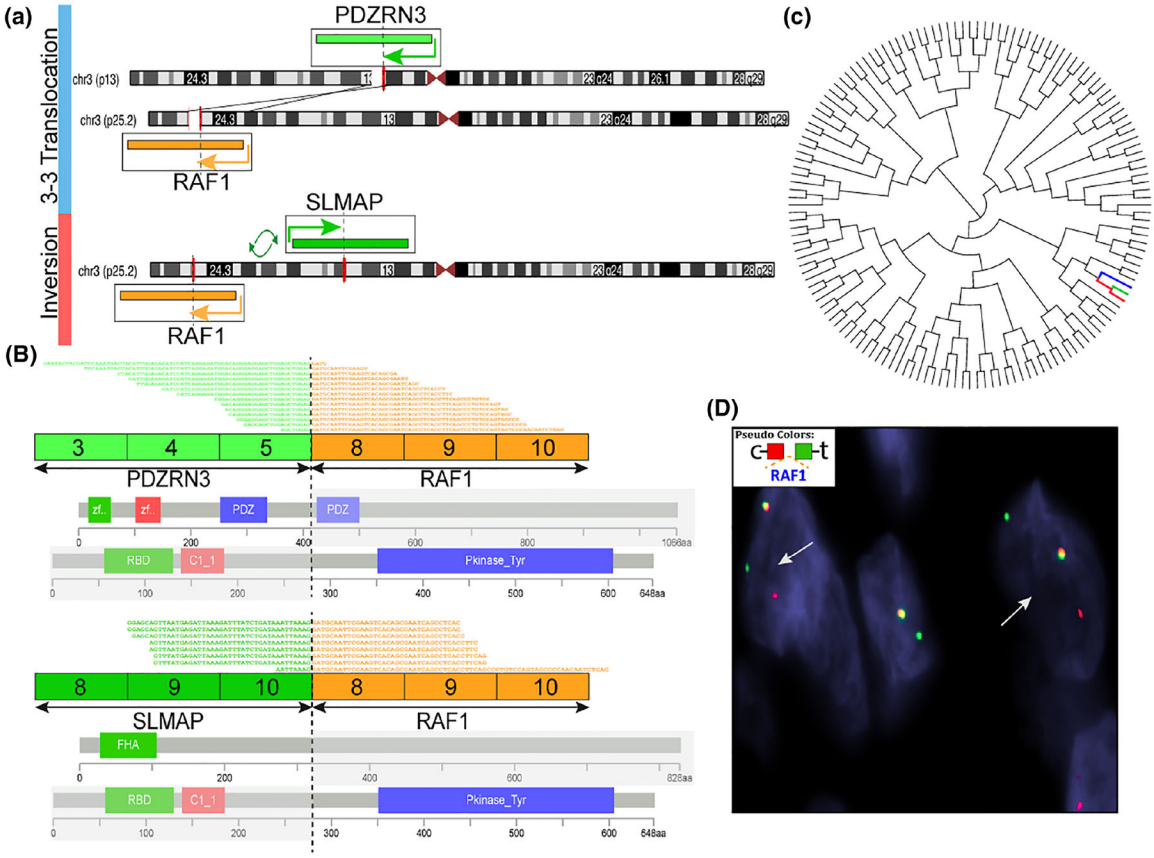

FIGURE 3.

RAF1 gene fusion structures and molecular correlates. A, Diagrammatic representation of 2 *RAF1* fusions variants by targeted RNA sequencing. Case 1 (upper level) showing a *t*(3;3) translocation, with the 2 gene partners *PDZRN3* on 3p13 and *RAF1* on *3p25.2* having the same directions of transcriptions (illustrated by arrows). In contrast, case 2 (lower level) shows the 2 gene partners *RAF1* and *SLMAP* (3p14.3) are in opposite directions of transcriptions; their fusion is a result of an intrachromosomal inversion (demonstrated by arrows). B, RNAseq reads revealed exon 8 of *RAF1* fused in frame to exon 5 *PDZRN3* (case 1, upper panel) or with exon 10 of *SLMAP* (case 2, lower panel). The predicted fusion oncoproteins in both cases included the kinase domain of *RAF1*, encoded by exons 8–17 (illustrated by blue bar, Pkinase_Tyr). C, Unsupervised hierarchical clustering using the same platform of targeted RNA sequencing data showed that these 2 *RAF1* rearranged sarcomas (red branch, *SLMAP-RAF1*; light-blue; *PDZRN3-RAF1*) clustered closely to a *BRAF* rearranged pediatric fibrosarcoma (dark-blue), reported previously by our group,[4] as compared to more than 100 various soft tissue tumors. D, FISH showing RAF1 gene break-apart signal (case 8, red, centromeric; green; telomeric)

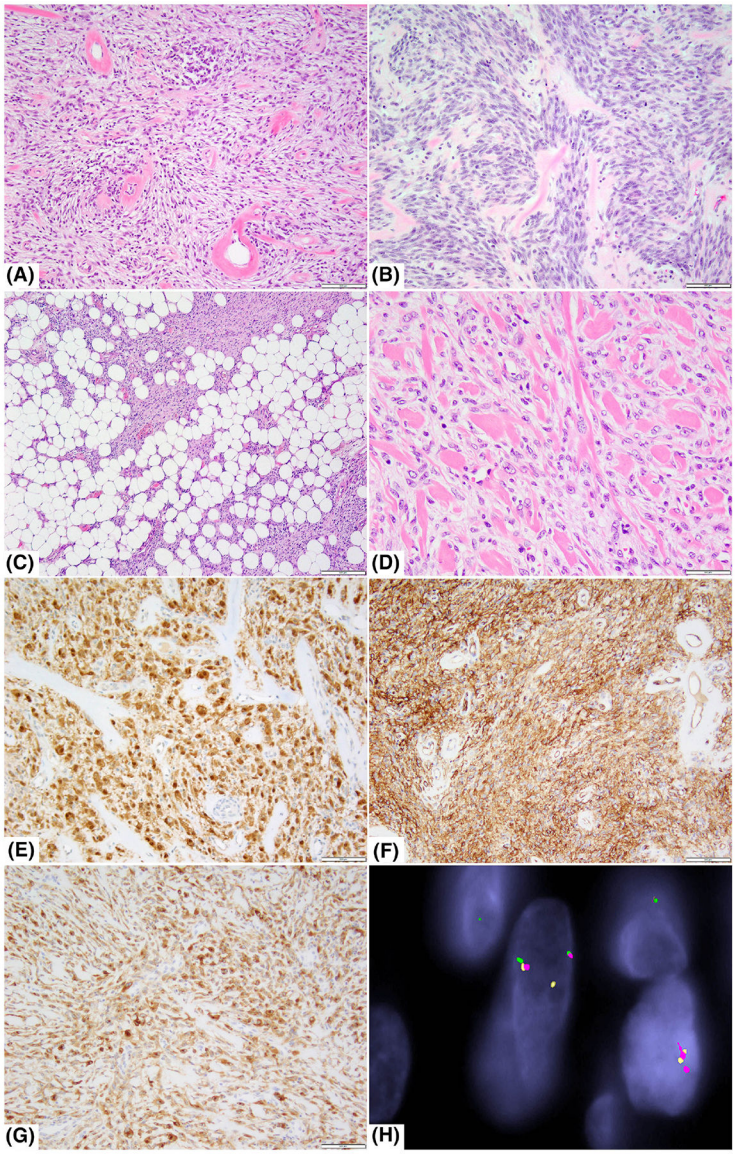

FIGURE 4.

Histologic and immunohistochemical features of *NTRK1*-rearranged tumors. A, Low cellularity maxillary bone tumor in a 13-year-old male showing haphazardly arranged bland spindle cells with striking perivascular rings of collagen (case 11, ×100). B, Tumor with increased cellularity in a 61-year-old female with a large pre-tibial deep soft tissue tumor showing short fascicles with interspersed band-like collagen (case 14; ×200). C, Superficial thigh mass in a 77-year-old female showing focal areas reminiscent of lipofibromatosis (case 22, ×40). D, Low cellularity thigh mass in a 15-year-old female showing abundant stromal band-like collagen (case 18, ×200). E,F, Immunohistochemical studies showing diffuse S100 and CD34 positivity (case 11; ×100). G, NTRK1 strong and diffuse immunoreactivity (case 18, ×100). H, FISH fusion assay shows the red signal (telomeric 5′-*TPM3*) comes together with the green signal (telomeric of 3′-*NTRK1*), while the orange signal (centromeric 5′-

NTRK1) breaks away from its green telomeric part, in keeping with a *TPM3–NTRK1* fusion (case 21)

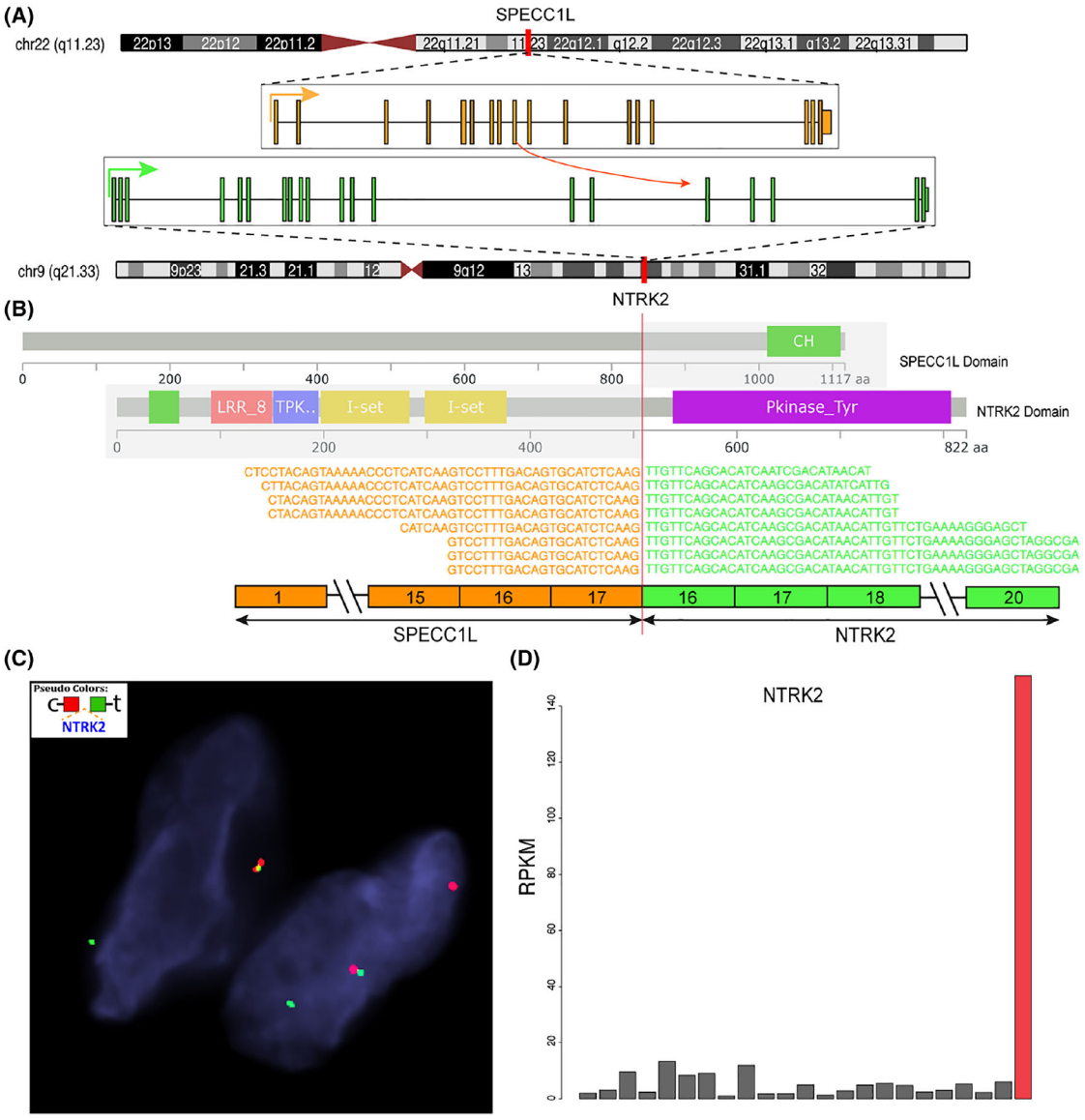

FIGURE 5.

SPECC1L–NTRK2 fusion structure and molecular correlates (case 25). A, Diagrammatic representation of *SPECC1L* on 22q11.23 fused to *NTRK2* on 9q21.33 (arrows show direction of transcription). B, RNAseq reads identified a fusion transcript composed of exon 17 of *SPECC1L* fused to exon 16 of *NTRK2*. Protein domains depiction of each gene showing the predicted fusion oncoprotein contains the kinase domain of NTRK2 (purple). C, FISH confirming the break-apart signal of NTRK2 (red, centromeric; green telomeric). D, Significant upregulation of *NTRK2* mRNA expression (red bar, case 25), compared to other sarcoma types available on the same targeted RNA sequencing platform

TABLE 1

RAF1/BRAF and NTRK1/2 rearranged tumors

	Age/sex	Location	Gene fusion/rearrangement	Cellularity	FU
Case 1	67/F	Abdomen	*PDZRN3-RAF1*[a]	IC	AWD (7 mo), lung, liver, and periton mets
Case 2	41/M	Thigh	*SLMAP-RAF1*[a]	LC	NA
Case 3	2/F	Rectum	*TMF1-RAF1*[b]	LC	NA
Case 4	45/F	Back	*RAF1*	LC	NED (36 mo)
Case 5	10/M	Thigh	*RAF1*	LC	NA
Case 6	38/F	Shoulder	*RAF1*	IC	NED (9 mo)
Case 7	27/F	Back	*RAF1*	LC	NED (26 mo)
Case 8	59/M	Chest wall	*RAF1*	IC	NED (25 mo), s/p RT
Case 9	48/F	Hand	*BRAF*	LC	AWD (22 mo) (persistent local disease)
Case 10	18/F	Thigh	*BRAF*	IC	NA
Case 11	13/M	Maxilla	*LMNA-NTRK1*	LC	NED (648 mo)
Case 12	4/M	Mandible	*LMNA-NTRK1*	LC	NED (144 mo, s/p LR, RT)
Case 13	16/F	Chest wall	*LMNA-NTRK1*	IC	NA
Case 14	61/F	Lower leg	*LMNA-NTRK1*	IC	DOO (375 mo), lung mets
Case 15	18/M	Stomach	*LMNA-NTRK1*	IC	DOD (25 mo)
Case 16	5/M	Leg	*LMNA-NTRK1*	LC	NED (3 mo)
Case 17	15/F	Thigh	*LMNA-NTRK1*	LC	NED (14 mo)
Case 18	15/F	Thigh	*LMNA-NTRK1*	LC	NA
Case 19	38/M	Wrist	*TPM3-NTRK1*[c]	LC	NED (16 mo)
Case 20	23/M	Arm	*TPM3-NTRK1*	IC	AWD (36 mo), lung and abd mets
Case 21	35/M	Chest wall	*TPM3-NTRK1*	LC	NA
Case 22	77/F	Thigh	*TPR-NTRK1*	LC	NA
Case 23	17/F	Chest wall	*NTRK1*	LC	NA
Case 24	3/M	Shoulder	*NTRK1*	LC	NA
Case 25	20/M	Forearm	*SPECC1L-NTRK2*[a]	LC	NA

Abbreviations: DOD, dead of disease; DOO, dead of other causes; IC, increased cellularity; LC, low cellularity; LR, local recurrence; mets, metastases; mo, months; NA, not available; NED, no evidence of disease; RT, radiation therapy.

[a] Targeted RNA sequencing.

[b] Foundation One.

[c] Archer DX.